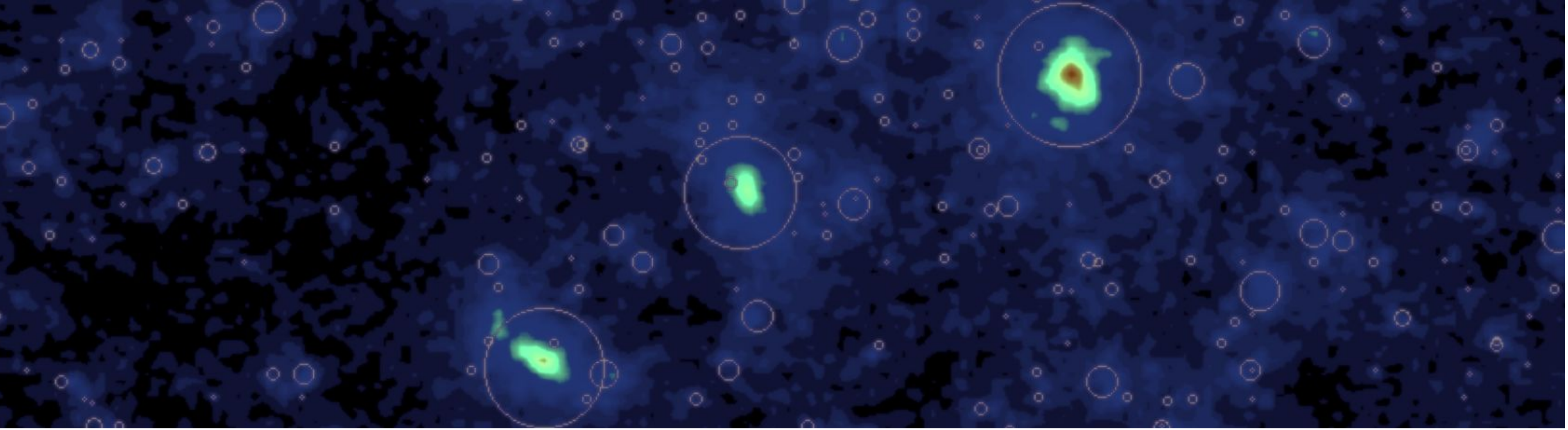

Cosmic Shear Cosmology Beyond 2-Point Statistics: A Combined Peak Count and Correlation Function Analysis of DES-Y1

Joachim Harnois-Déraps[1,2★], Nicolas Martinet[3], Tiago Castro[4,5,6,7], Klaus Dolag[8,9], Benjamin Giblin[2], Catherine Heymans [2,10], Hendrik Hildebrandt[10] & Qianli Xia[2]

https://arxiv.org/abs/2012.02777

Many slides are a courtesy Nicolas Martinet

Why go beyond?

With 2PCF, the Density field is summarized as:

$$\langle\delta(\mathbf{k})\delta(\mathbf{k}')\rangle = (2\pi)^3\delta_D(\mathbf{k}-\mathbf{k}')P(\mathbf{k})$$

$$\delta(\mathbf{x}) = \sum \tilde{\delta}(\mathbf{k})\exp(i\mathbf{k}\cdot\mathbf{x}).$$

$$\tilde{\delta}(\mathbf{k}) = |\tilde{\delta}(\mathbf{k})|\exp(i\phi_{\mathbf{k}})$$

We are ignoring the cosmological information contained in these phases!

$$\boxed{D_k \equiv \phi_{k+1} - \phi_k}$$

Goal: access phase information with non-Gaussian statistics

These 2 snapshots have the same P(k)!

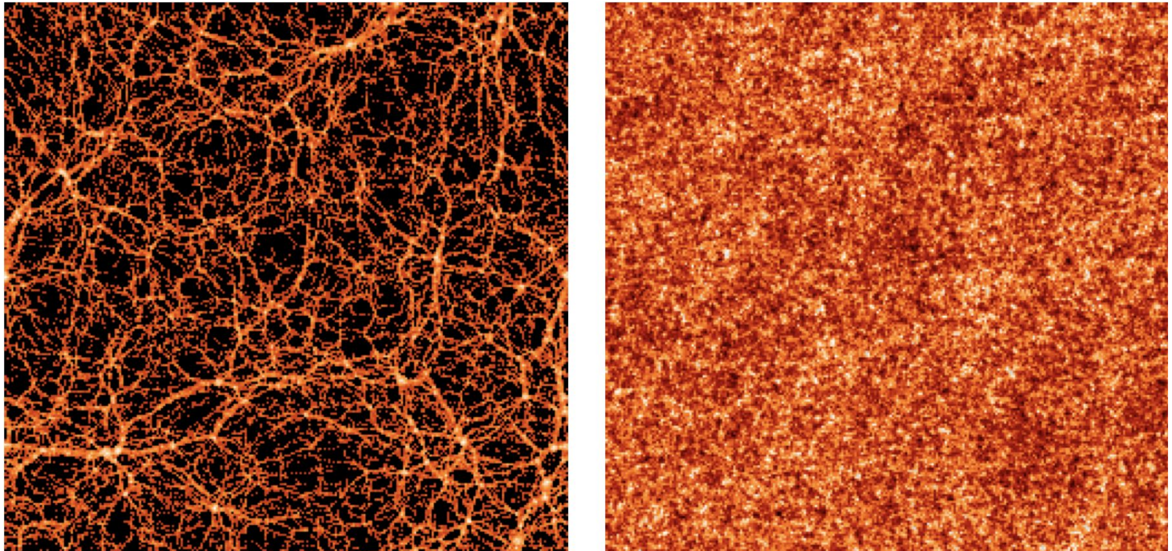

Coles & Chiang, Nature, Volume 406, Issue 6794, pp. 376-378 (2000)

What is to gain: Dark Matter+Dark Energy

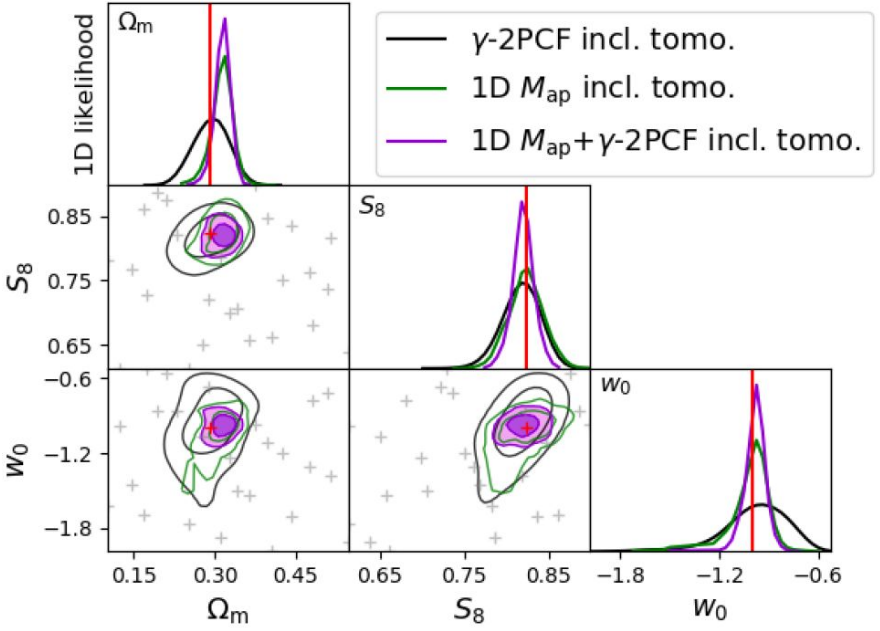

Martinet+(2020), https://arxiv.org/abs/2010.07376

- Forecasts for 100 deg² of Euclid with a 5-slice tomography
- Constraints from PDF + shear 2PCF on w_0 are *3x smaller* than 2PCF alone, *2x smaller* for S_8)
- *Huge potential for DE*

What is to gain: Neutrino Mass

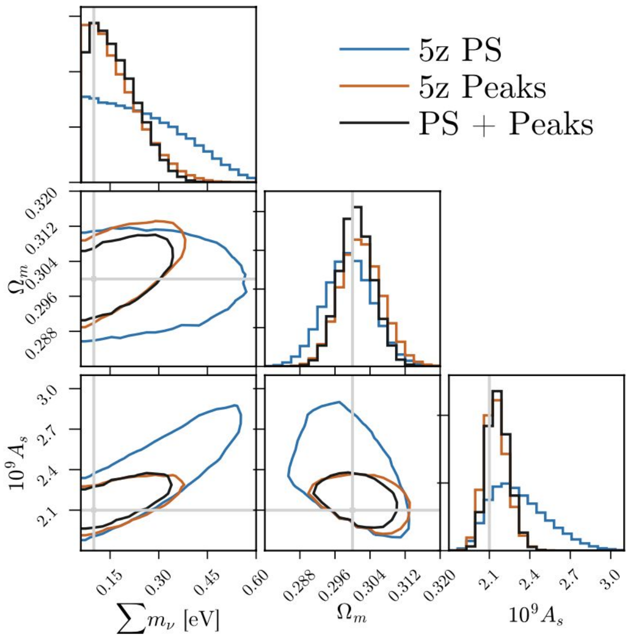

Li+(2019), PRD, 99f, 3527

- Forecasts for LSST
- Constraints from Peaks + shear C_ell on M_nu are *50% smaller*)

Cosmology with shear 2PCF

Observations

Ellipticities (ϵ_1, ϵ_2)

Estimator: shear 2PCF

$$\hat{\xi}_{\pm}^{ij}(\theta) = \frac{\sum_{ab} w_a w_b \left[\epsilon_t^i(\vec{x}_a)\epsilon_t^j(\vec{x}_b) \pm \epsilon_\times^i(\vec{x}_a)\epsilon_\times^j(\vec{x}_b)\right]}{\sum_{ab} w_a w_b}$$

Tomography

Redshifts (z)

Calibration (spectroscopic, SOM, BPZ...)

Redshift distribution: n(z)

Systematic biases

- Shear calibration
- Mean redshift
- Intrinsic alignment
- Baryons
- etc

Cosmological parameters (e.g. Ω_m, σ_8)

Theoretical predictions

$$\xi_{\pm}^{ij}(\theta) = \frac{1}{2\pi}\int d\ell\,\ell\,P_\kappa^{ij}(\ell)\,J_{0,4}(\ell\theta)$$

$$P_\kappa^{ij}(\ell) = \int_0^{\chi_H} d\chi\,\frac{q_i(\chi)q_j(\chi)}{[f_K(\chi)]^2}\,P_\delta\left(\frac{\ell}{f_K(\chi)},\chi\right)$$

Cosmology with mass maps

Observations

Ellipticities $(\varepsilon_1, \varepsilon_2)$

Redshifts (z)

Tomography

Calibration (spectroscopic, SOM, BPZ...)

Estimator:
mass map statistics

Redshift distribution: n(z)

Systematic biases
- Shear calibration
- Mean redshift
- Intrinsic alignment
- Baryons
- etc

Cosmological parameters (e.g. Ω_m, σ_8)

~~Theoretical predictions~~
Model from N-body simulations

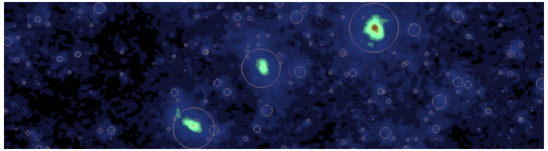

Cosmology with mass maps

This paper:

Systematic biases
- Shear calibration
- Mean redshift
- Intrinsic alignment
- Baryons
- etc

Ellipticities (ϵ_1, ϵ_2)

Estimator:
Peak count statistics

Observations

Tomography

Redshifts (z)

Calibration (spectroscopic, SOM, BPZ...)

Redshift distribution: n(z)

Cosmological parameters (e.g. Ω_m, σ_8)

~~Theoretical predictions~~
Model from N-body simulations

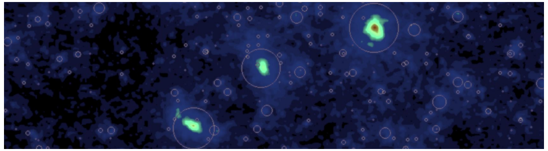

Cosmological Inference

-Data: DES-Y1 (public)

-Model: cosmo-SLICS (JHD+2019)

-Covariance matrix: SLICS (JHD+2018)

-Likelihood: cosmoSIS

$$\mathcal{L}(\boldsymbol{\pi}|\boldsymbol{d}) \propto \frac{N_{\rm sim}}{2}\ln\left[1+\chi^2/(N_{\rm sim}-1)\right]$$

Sellentin & Heavens (2016)

DES-Y1 Mosaic

18 tiles or 100 sq. deg. each

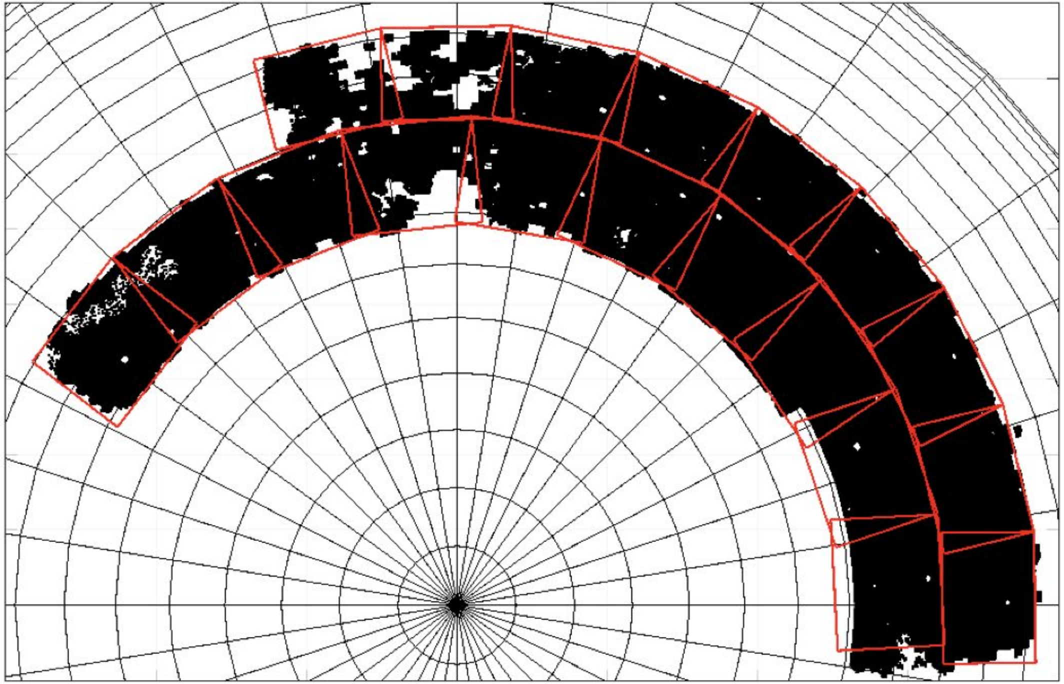

Data:

tomo	Z_B range	No. of objects	$n_{\rm eff}$	σ_ϵ	$\langle z_{\rm DIR}\rangle$
bin1	0.20 – 0.43	6,993,471	1.45	0.26	0.403 ± 0.008
bin2	0.43 – 0.63	7,141,911	1.43	0.29	0.560 ± 0.014
bin3	0.63 – 0.90	7,514,933	1.47	0.26	0.773 ± 0.011
bin4	0.90 – 1.30	3,839,717	0.70	0.27	0.984 ± 0.009

Sims:

Sim. suite	$L_{\rm box}$	$n_{\rm p}$	$N_{\rm sims}$	$N_{\rm LC}$	$N_{\rm cosmo}$
cosmo-SLICS	505	1536^3	52	520	26
SLICS	505	1536^3	124	124	1
SLICS-HR	505	1536^3	5	50	1
Magneticum 2	352	2×1583^3	1	10	1
Magneticum 2b	640	2×2880^3	1	10	1

parameter	$\Omega_{\rm m}$	S_8	h	w_0
sampling	[0.1, 0.55]	[0.6, 0.9]	[0.6, 0.82]	[-2.0, -0.5]

Model: wCDM simulations

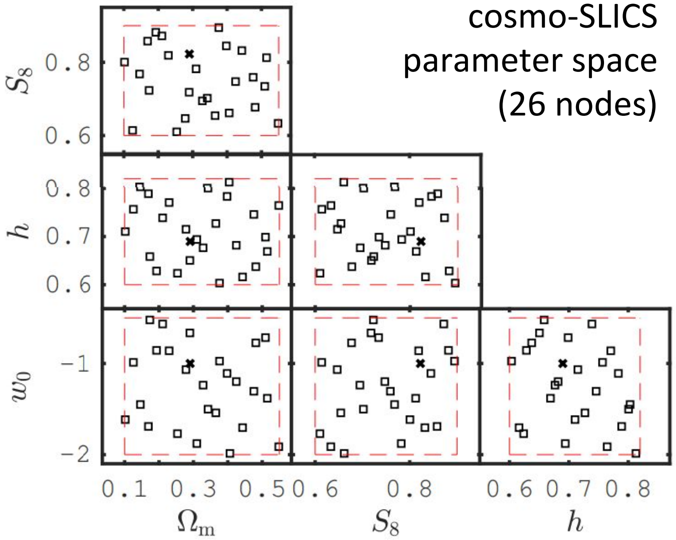

- Ray-trace the N-body suite
- Assign the 4 DES-Y1 redshift bins
- Use the positions, shapes (|e|) and responsivity per object
- Measure Peak Function dN/d(SNR)
- Interpolate with a Gaussian Processes Regression Emulator

Covariance: LCDM simulations

- 1240 surveys (124 independent sims x 10 shape noise realisations)

Data vector : Peaks

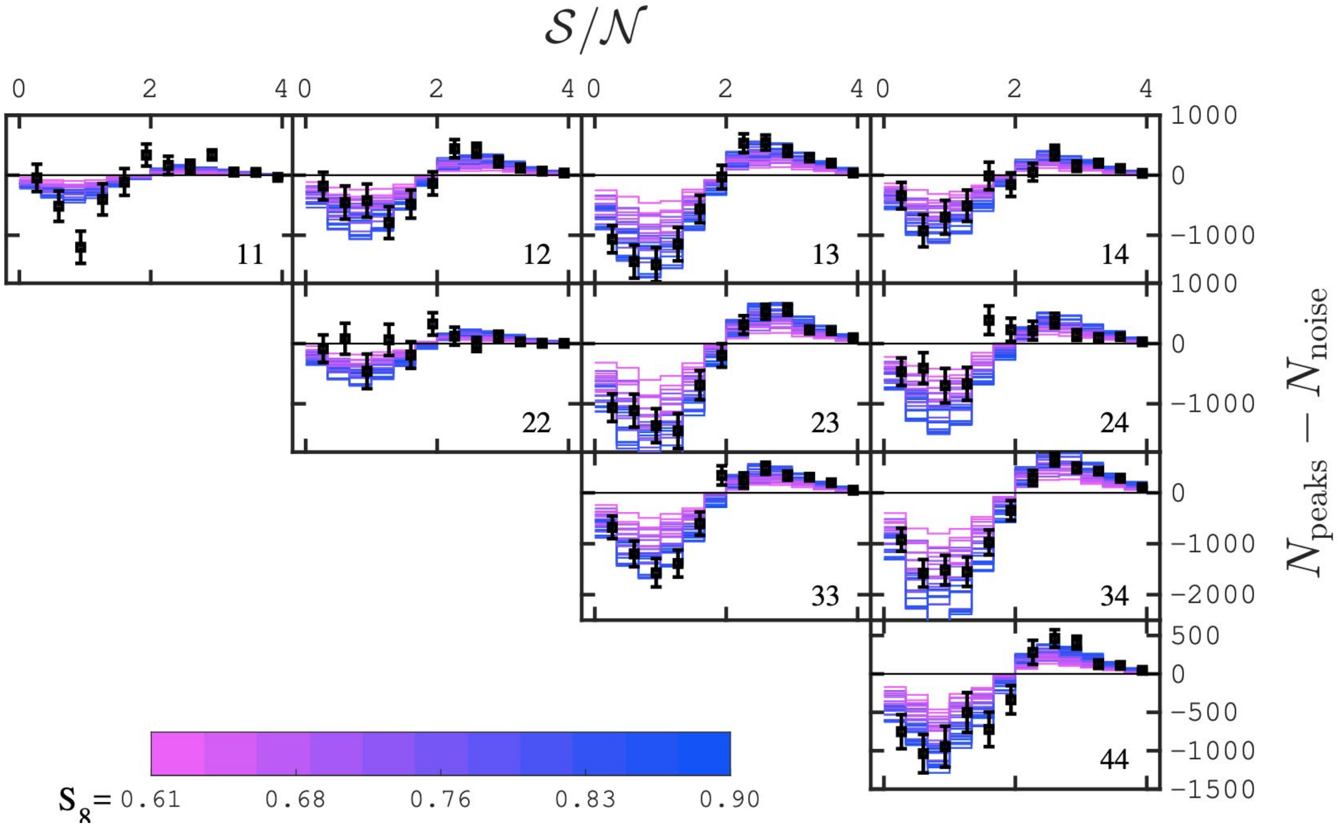

Systematics

Interpolation error from the GPR

Photometric redshifts uncertainty

Shear calibration bias

Mass resolution

Baryonic feedback

Intrinsic alignments of galaxies

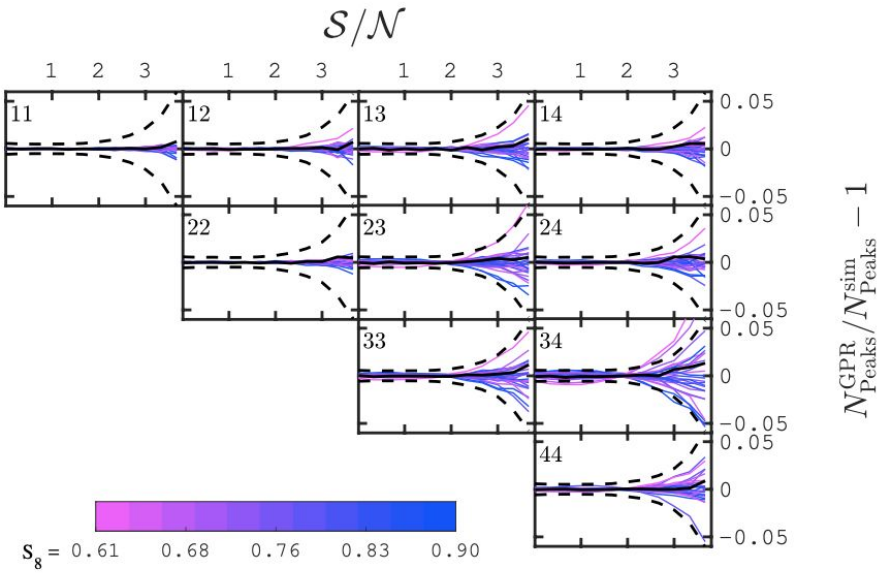

Systematics

Interpolation error from the GPR

Photometric redshifts uncertainty

Shear calibration bias

Mass resolution

Baryonic feedback

Intrinsic alignments of galaxies

Model with ray-tracing:

Sample 10 shifts in dm and dz

Fit each bin with a linear model

Compute dN/d(dz) and dN/d(dm)

Marginalise in cosmoSIS

Systematics

Interpolation error from the GPR

Photometric redshifts uncertainty

Shear calibration bias

Mass resolution

Baryonic feedback

Intrinsic alignments of galaxies

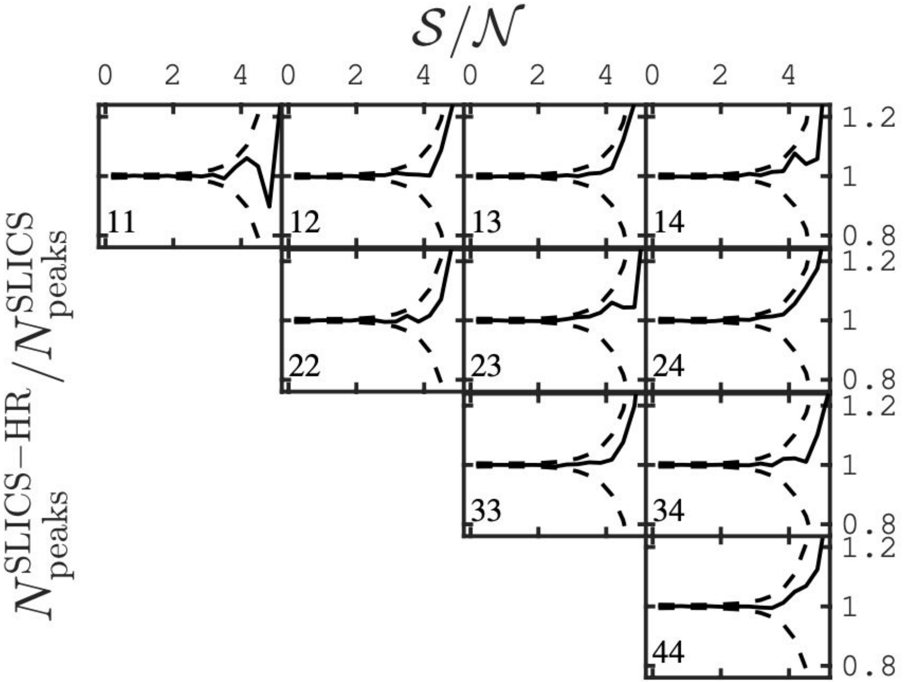

Systematics

Interpolation error from the GPR

Photometric redshifts uncertainty

Shear calibration bias

Mass resolution

Baryonic feedback

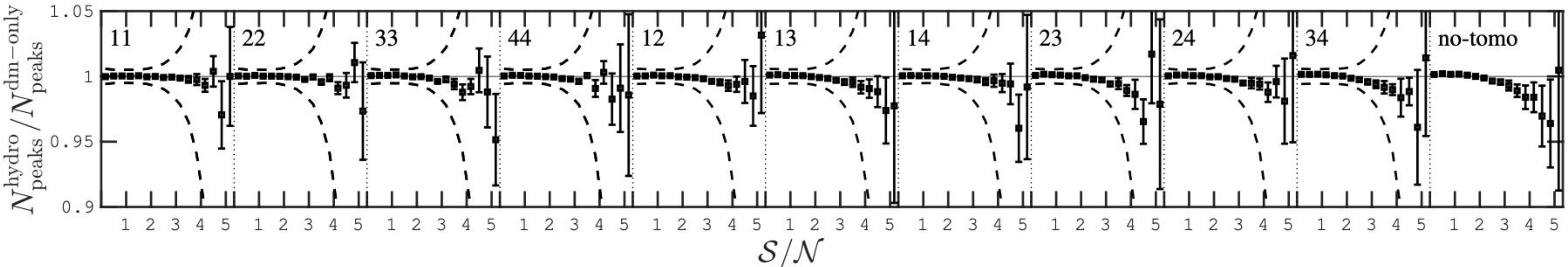

Systematics

Interpolation error from the GPR

Photometric redshifts uncertainty

Shear calibration bias

Mass resolution

Baryonic feedback

Intrinsic alignments of galaxies

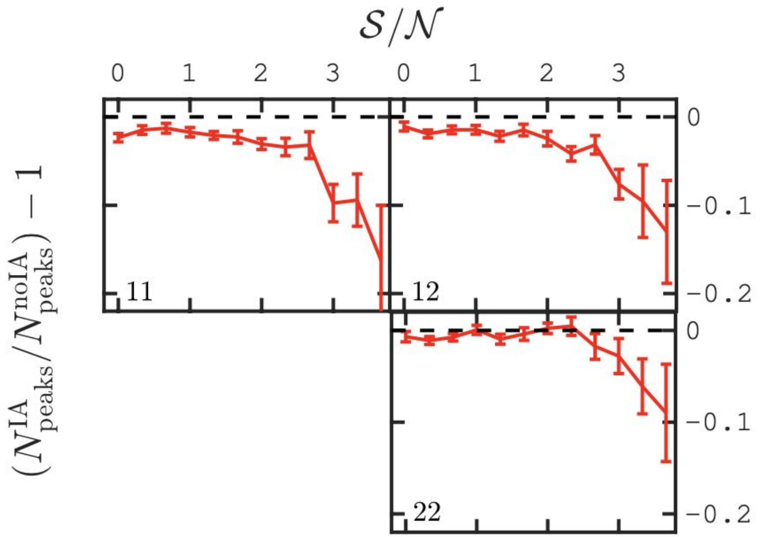

Systematics

Interpolation error from the GPR

Photometric redshifts uncertainty

Shear calibration bias

Mass resolution

Baryonic feedback

Intrinsic alignments of galaxies

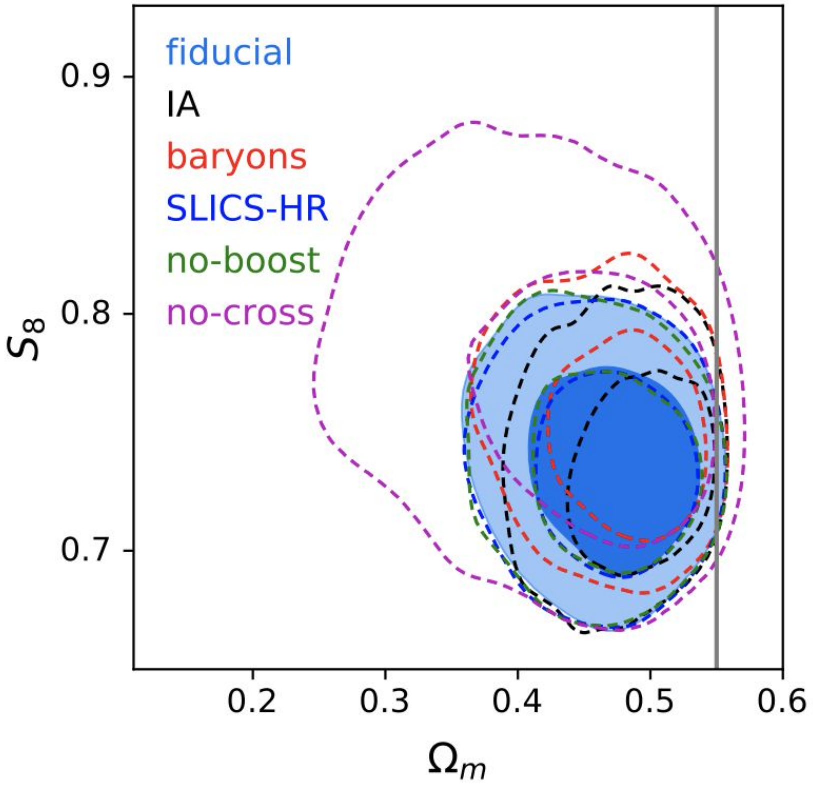

Results:

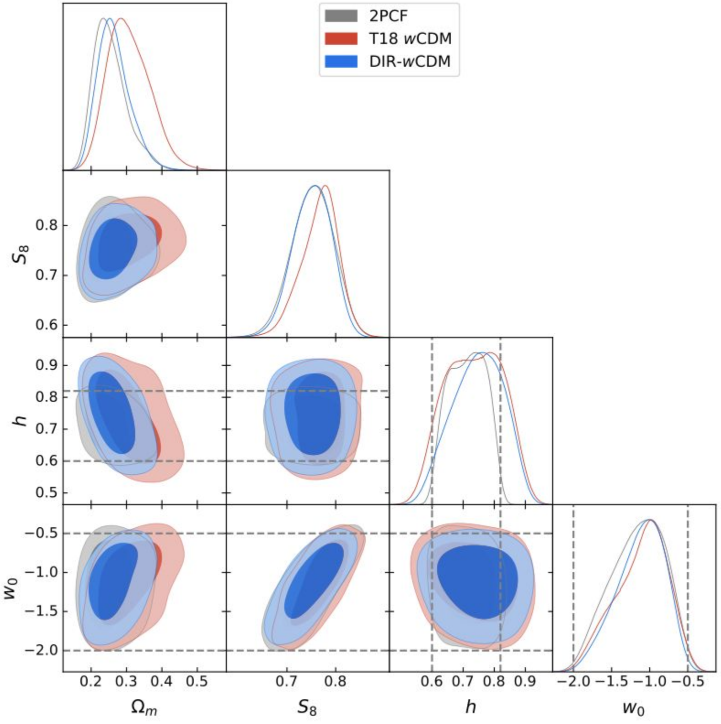

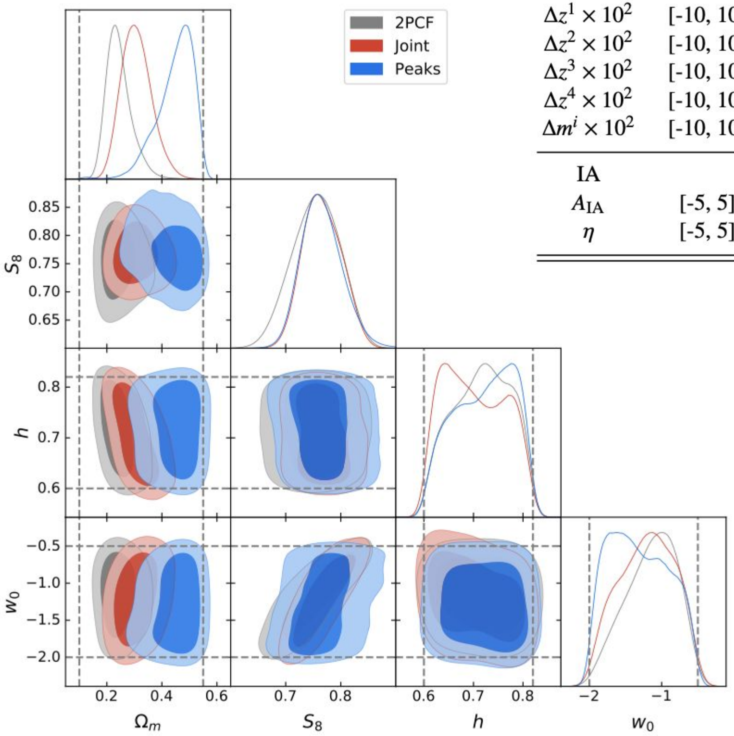

Parameter	range	prior
Cosmology		
$\Omega_{\rm m}$	[0.1, 0.55]	Flat
σ_8	[0.53, 1.3]	Flat
h	[0.6, 0.82]	Flat
w_0	[-2.0, -0.5]	Flat
Nuisance		
$\Delta z^1 \times 10^2$	[-10, 10]	$\mathcal{G}(0, 0.8)$
$\Delta z^2 \times 10^2$	[-10, 10]	$\mathcal{G}(0, 1.4)$
$\Delta z^3 \times 10^2$	[-10, 10]	$\mathcal{G}(0, 1.1)$
$\Delta z^4 \times 10^2$	[-10, 10]	$\mathcal{G}(0, 0.9)$
$\Delta m^i \times 10^2$	[-10, 10]	$\mathcal{G}(1.2, 1.3)$
IA		
$A_{\rm IA}$	[-5, 5]	Flat
η	[-5, 5]	Flat

Results:

	pipeline	S_8	Ω_m
Fiducial	Peaks	$0.780^{+0.019}_{-0.056}$	-
	2PCF	$0.753^{+0.043}_{-0.043}$	$0.254^{+0.033}_{-0.056}$
	Joint	$0.766^{+0.033}_{-0.038}$	-
Variations	2PCF (T18, *w*CDM)	$0.797^{+0.037}_{-0.037}$	$0.290^{+0.079}_{-0.051}$
	2PCF (DIR-*w*CDM)	$0.752^{+0.042}_{-0.037}$	$0.264^{+0.035}_{-0.054}$
	2PCF (ΛCDM)	$0.761^{+0.027}_{-0.027}$	$0.272^{+0.031}_{-0.056}$
	2PCF (T18, ΛCDM)	$0.792^{+0.032}_{-0.021}$	$0.304^{+0.038}_{-0.062}$
	2PCF (J20, ΛCDM)	$0.765^{+0.036}_{-0.031}$	$0.252^{+0.041}_{-0.086}$
	Peaks (cross-tomo, with IA)	$0.735^{+0.024}_{-0.032}$	-
	Peaks (cross-tomo, with baryons)	$0.750^{+0.026}_{-0.031}$	-
	Peaks (cross-tomo, with SLICS-HR)	$0.734^{+0.025}_{-0.032}$	-
	Peaks (cross-tomo, no-boost)	$0.736^{+0.025}_{-0.032}$	-
	Peaks (cross-tomo)	$0.737^{+0.027}_{-0.031}$	-
	Joint (cross-tomo)	$0.743^{+0.024}_{-0.024}$	-
Mocks	Peaks (cross-tomo, no syst)	$0.787^{+0.024}_{-0.024}$	$0.325^{+0.054}_{-0.067}$
	Peaks (cross-tomo)	$0.776^{+0.045}_{-0.045}$	$0.297^{+0.048}_{-0.066}$
	2PCF (FID)	$0.772^{+0.042}_{-0.042}$	$0.314^{+0.049}_{-0.070}$

Conclusions: Map statistics are powerful!

- 1D Map outperforms peaks, voids, and shear-2PCF
- Tomography with cross-bins improves the forecast precision by 50% compared to previous tomography
- 1D Map + shear-2PCF is twice better than shear-2PCF alone on the S8 forecast precision
- First combined forecasts on w_0: 1D Map + shear-2PCF almost three times better than shear-2PCF
- Next: Baryons and IA (ongoing). If we want to get serious about this, we need to list the requirements for percent level accuracy, estimate the resources needed for new simulations, and establish a road map.

Additional Slides

Covariance Matrix

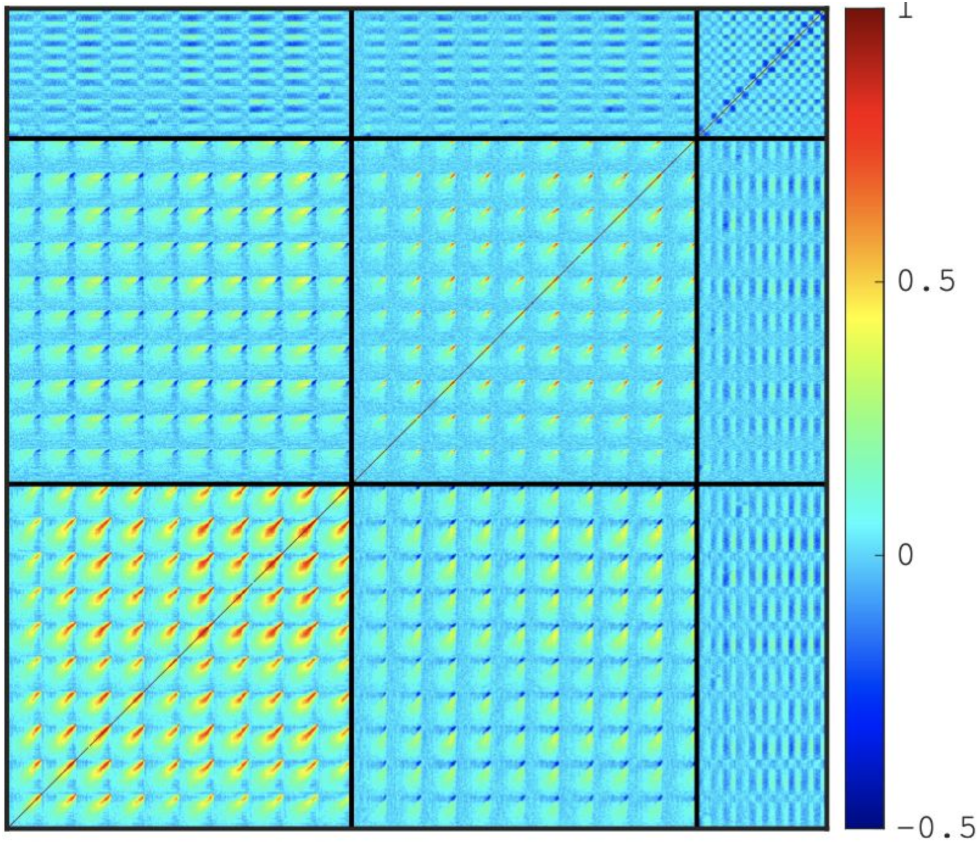

Data vector : 2PCF

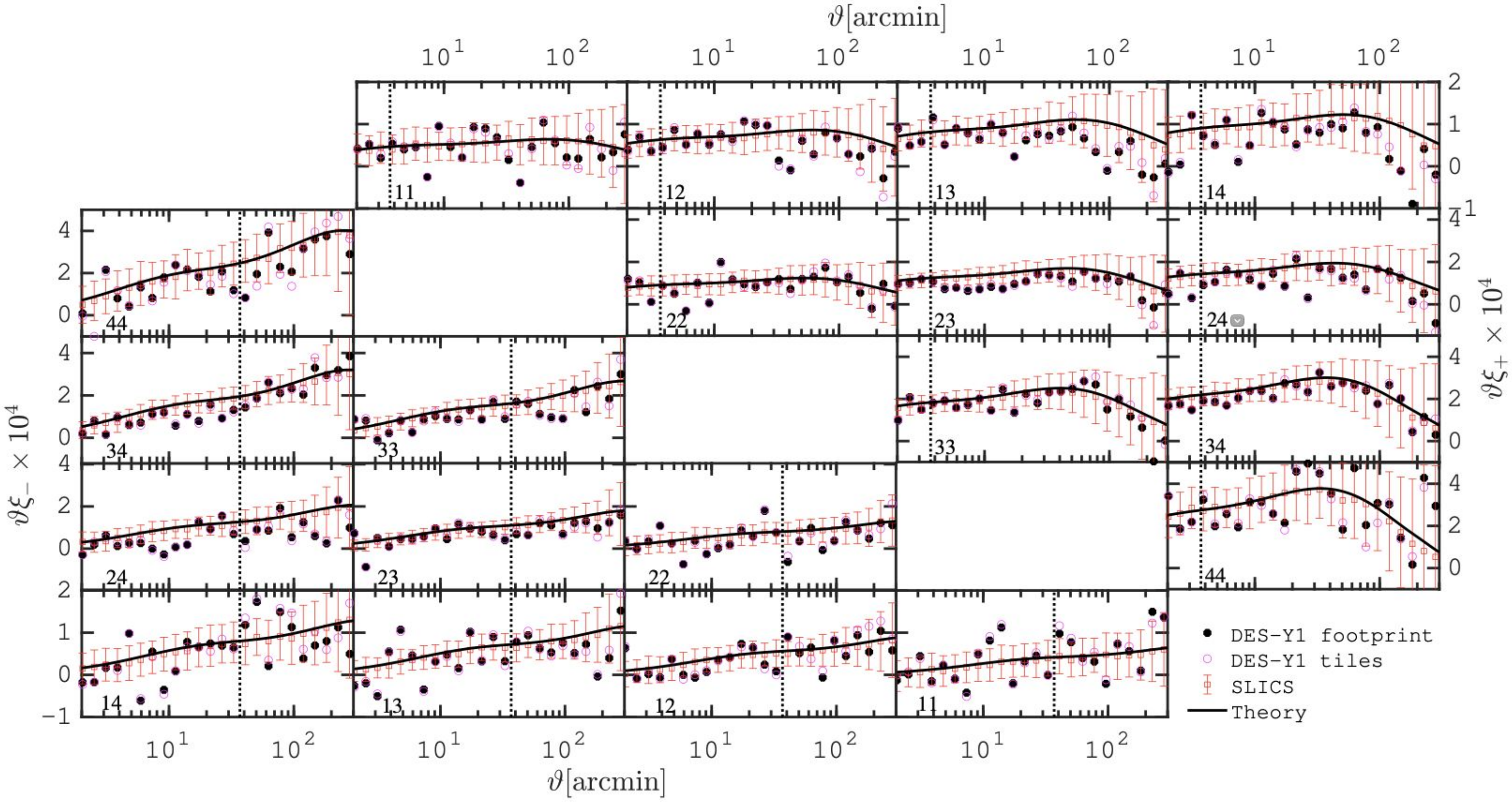

Aperture mass map

$$M_{\mathrm{ap}}(\boldsymbol{\theta}_0) = \frac{1}{n_{\mathrm{gal}}} \sum_i Q(|\boldsymbol{\theta}_i - \boldsymbol{\theta}_0|)\epsilon_{\mathrm{t}}(\boldsymbol{\theta}_i, \boldsymbol{\theta}_0)$$

$$\epsilon_{\mathrm{t}}(\boldsymbol{\theta}, \boldsymbol{\theta}_0) = -\Re\left[\, \hat{\epsilon}(\boldsymbol{\theta})\, \mathrm{e}^{-2\mathrm{i}\phi(\boldsymbol{\theta}, \boldsymbol{\theta}_0)} \,\right]$$

$$\sigma(M_{\mathrm{ap}}(\boldsymbol{\theta}_0)) = \frac{1}{\sqrt{2} n_{\mathrm{gal}}} \left(\sum_i |\hat{\epsilon}(\boldsymbol{\theta}_i)|^2 Q^2(|\boldsymbol{\theta}_i - \boldsymbol{\theta}_0|) \right)^{1/2}$$

$$\frac{S}{N}(\boldsymbol{\theta}_0) = \frac{\sqrt{2} \sum_i Q(|\boldsymbol{\theta}_i - \boldsymbol{\theta}_0|)\epsilon_{\mathrm{t}}(\boldsymbol{\theta}_i, \boldsymbol{\theta}_0)}{\sqrt{\sum_i |\hat{\epsilon}(\boldsymbol{\theta}_i)|^2 Q^2(|\boldsymbol{\theta}_i - \boldsymbol{\theta}_0|)}}$$

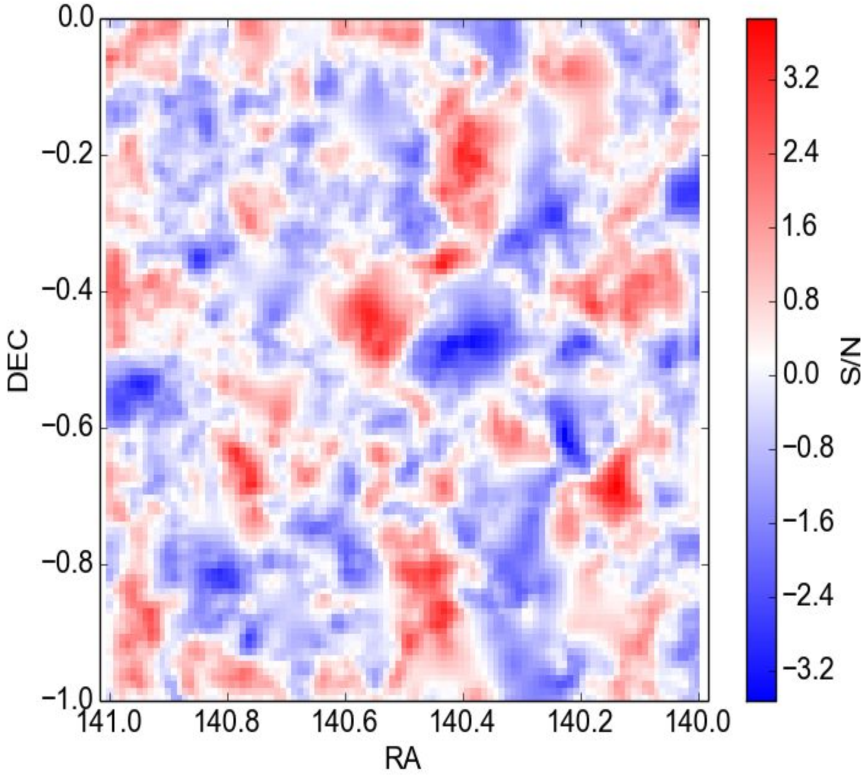

DES-Yr3 peak prediction with tomography
(Zürcher et al. 2020)

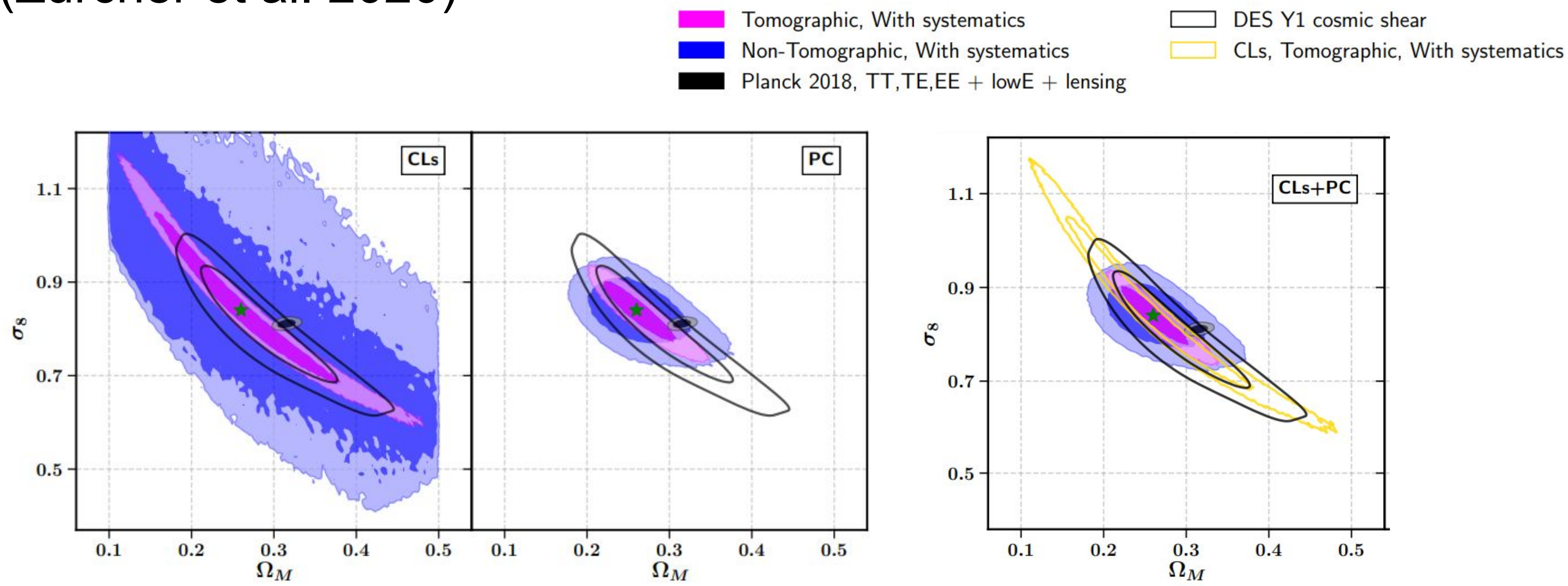

- Constraints on S8 improved by 25% with tomography
- Here, tomography works better for 2PCF than peaks *because of redshift bin cross-correlations*